LETTER

Fully differential study of few-body dynamics in multi-electron atomic fragmentation processes

To cite this article: Y Gao et al 2017 J. Phys. B: At. Mol. Opt. Phys. 50 10LT01

View the article online for updates and enhancements.

Related content

- Role of elastic scattering in inelastic atomic fragmentation processes

 M Schulz
- Comparative study of single and double ionization of helium by ion impact D Fischer, M Schulz, R Moshammer et al.
- Fully differential cross sections for the single ionization of He by ion impact
 D Fischer, R Moshammer, M Schulz et al.



Fully differential study of few-body dynamics in multi-electron atomic fragmentation processes

1

Y Gao¹, S F Zhang¹, M Schulz², X L Zhu¹, R T Zhang¹, W T Feng¹, D L Guo¹, D M Zhao¹ and X Ma¹

E-mail: x.ma@impcas.ac.cn

Received 5 January 2017, revised 18 March 2017 Accepted for publication 24 March 2017 Published 27 April 2017



Abstract

We have measured fully momentum analyzed Ar^{3+} recoil ions and two ejected electrons as well as He^+ projectiles in coincidence with each other for 30 keV amu $^{-1}$ He^{2+} + Ar collisions. Fully differential cross sections for electron transfer from the target to the projectile accompanied by the ejection of two additional target electrons were extracted. To a large extent the data can be reproduced by an independent electron model. However, we also observed a surprisingly strong correlation between the electron momenta and the projectile momentum transfer.

Keywords: fully differential, transfer ionization, strong correlation, few-body dynamics

(Some figures may appear in colour only in the online journal)

One of the most important goals of atomic physics research is to advance our understanding of few-body dynamics in atomic systems containing at least three mutually interacting particles [1, 2]. This represents an enormous theoretical challenge because it is well established that for such atomic systems the Schrödinger equation is not analytically solvable although the underlying forces acting between the particles are very well understood. Therefore, detailed experiments testing theoretical modelling efforts are crucial, where kinematically complete experiments offer the most sensitive tests.

Experiments studying ionization processes are particularly suitable to test few-body dynamics because here the final state involves at least three unbound particles (the scattered projectile, the ejected electron(s) and the recoiling target ion). So far, kinematically complete experimental studies on such processes were focused on pure single ionization (SI) of the target (for reviews see e.g. [3, 4]). For electron impact a solid understanding of the collision dynamics has emerged even at small energies (e.g. [1, 5, 6]), however, ion impact studies are much more challenging both theoretically and experimentally

due to the larger projectile mass [4]. For transfer ionization (TI), i.e. the capture of one target electron to the projectile and the ejection of a second target electron, numerous kinematically complete experiments were reported as well [e.g. 7–12]. However, here too, like in SI, the final state only involves three unbound particles. Therefore, kinematically, the complexity of few-body dynamics in this process is only enhanced to some extent compared to SI. For double ionization (leading to four unbound particles in the final state) kinematically complete data were reported for electron impact (e.g. [13, 14]). For ion impact, such experiments are much more challenging and here, only one nearly kinematically complete experiment was reported [15]. Multiply differential data are also available for triple ionization by ion impact [16], but there the measured cross sections nevertheless represent an integration of the fully differential cross sections (FDCS) over several kinematic parameters.

In this letter we present measured FDCS for the transfer of one electron to the projectile with simultaneous ejection of two additional target electrons (to which we refer as T1I2) in

¹ Institute of Modern Physics, Chinese Academy of Sciences, Lanzhou 730000, People's Republic of China

² Department of Physics and LAMOR, Missouri University of Science & Technology, Rolla, Missouri 65409, United States of America



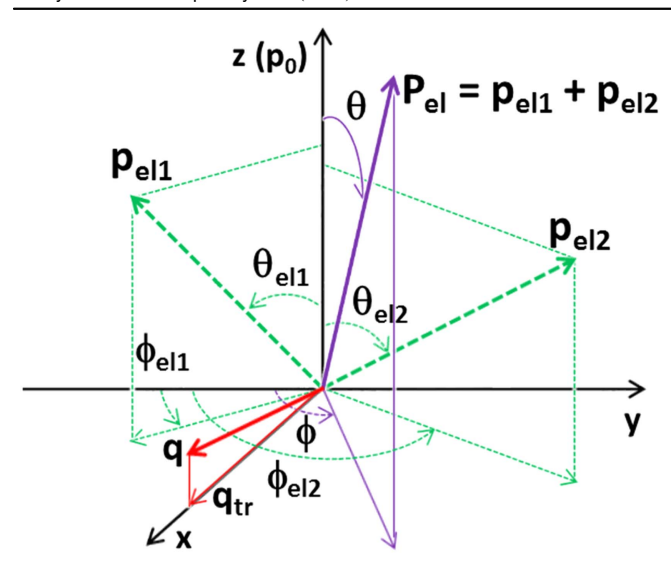


Figure 1. An illustration of the collision geometry and the coordinate system used in the data analysis. For the details, see text.

collisions of 30 keV amu⁻¹ He²⁺ with Ar. This process is kinematically more complex than SI as the final state involves four unbound particles. At the same time, the transfer step selects, on average, much closer collisions than what is expected for pure target double ionization (DI). As a result, we expected the interaction between the two nuclei in the system (NN interaction) to have a much larger impact on fewbody dynamics compared to DI. With this higher degree of complexity and enhanced role played by the NN interaction, we anticipated major differences in the FDCS between T1I2 and SI. Instead, some of the features in the measured FDCS bore a remarkable and surprising resemblance to the FDCS for SI. Nevertheless, we also observed some important differences in the FDCS for both processes, reflecting the qualitative differences in few-body dynamics.

The experiment was performed at the 320 kV platform for multidisciplinary research with highly charged ions at the Institute of Modern Physics, Lanzhou, China. Briefly, 30 keV amu⁻¹ He²⁺ ion beams, delivered by the platform, are well-collimated and intersect with a supersonic argon gas jet at the center of a reaction microscope [17]. The produced fragments (electrons and recoil ion) are extracted by a weak electrostatic field (1.77 V cm⁻¹) and a homogeneous magnetic field (11 G) perpendicular to both the projectile and the jet directions and are projected onto two position-sensitive detectors, mounted along the axis of the extraction field and facing each other. The scattered beam was charge-state analyzed by an electrostatic deflector downstream from the collision center, and the He⁺ ions were directed to a position sensitive detector while the remaining primary beam was collected by a Faraday cup. The recoil ion, two emitted electrons and the charge-exchanged projectile were measured in quadruple coincidence so that the various reaction channels could be distinguished. The momenta of the target fragments were obtained from the detector position and coincidence time information in the off-line analysis (for details see [17]). In figure 1 we illustrate the collision geometry and the coordinate system that we used to present the dependence of the measured multiple differential cross sections as a function of the electron ejection angles. The x-direction is defined by the transverse component of the momentum transfer q from the projectile to the target and the z-direction by the initial projectile momentum. The y-axis is, of course, perpendicular to the xz-plane. The momenta of the two ejected electrons are represented by the arrows labelled p_{el1} and p_{el2} , while the sum of both momenta is represented by the arrow labelled P_{el} . For each momentum the polar angle θ is measured relative to the z-axis and the azimuthal angle ϕ is, somewhat unconventionally, the angle between the negative y-axis and the projection of the momentum vector onto the xy-plane.

We start the discussion of the data by first analyzing the vector sum of both ejected electron momenta $\mathbf{P_{el}} = \mathbf{p_{el1}} + \mathbf{p_{el2}}$ (a similar analysis was performed for DI of Mg by electron impact [18]). In figure 2 three-dimensional angular distributions (3D-plots) of $\mathbf{P_{el}}$ are plotted as a function of the polar angle θ (horizontal axis) and the azimuthal angle ϕ .

For the spectrum in the left panel, the sum energy of both electrons was fixed at $\Sigma E_{\rm el}=10\pm3~{\rm eV}$ and the transverse momentum transfer at $q_{\rm tr}=5\pm1~{\rm a.u.}$ For the spectrum in the right panel, the corresponding values are $\Sigma E_{\rm el}=50\pm7.5~{\rm eV}$ and $q_{\rm tr}=15\pm3~{\rm a.u.}$ Since the positive x-axis is determined by the direction of ${\bf q_{tr}}$, the angles $\phi=90^{\circ}$ and 270° represent the two semi-planes containing ${\bf q_{tr}}$ and $-{\bf q_{tr}}$, respectively, as well as the initial beam axis. These two semi-planes combined to form the scattering plane which spanned the initial projectile momentum ${\bf p_0}$ and ${\bf q}$.

Before we discuss the features seen in figure 2, we recall what is typically observed in the corresponding 3D-plots for SI. There, the observed shapes of these spectra are usually remarkably simple: they consist of a double lobe structure with one maximum (known as the binary peak)³, occurring near the direction of \mathbf{q} (i.e. $\phi = 90^{\circ}$ and $\theta = [0, 90^{\circ}]$) and the second maximum (recoil peak), near the direction of $-\mathbf{q}$ (i.e. $\phi = 270^{\circ}$ and $\theta = [90^{\circ}, 180^{\circ}]$) [1, 4, 19, 20]. At projectile charge to speed ratios, η significantly larger than 1, a third peak structure was observed in the forward direction ($\theta = 0$) [21, 22]. Furthermore, the recoil peak tends to be considerably smaller than the binary peak and decreases in intensity (relative to the binary peak) with increasing \mathbf{q} .

Now turning back to the 3D plots for T1I2, we first emphasize that the disadvantage of analyzing P_{el} is that any information about the effect of electron–electron correlations on few-body dynamics is lost because the interaction between both electrons merely exchanges momentum between both particles internally (in other words, in the 3D plots of figure 2 both electrons are effectively treated as a single quasi-particle). The comparison between such plots for T1I2 and SI therefore primarily provides information on the effect of the capture step on collision dynamics.

³ This name is somewhat misleading as it suggests that it results from a binary interaction between only two particles. However, even when multiple interactions are important this peak structure is preserved.



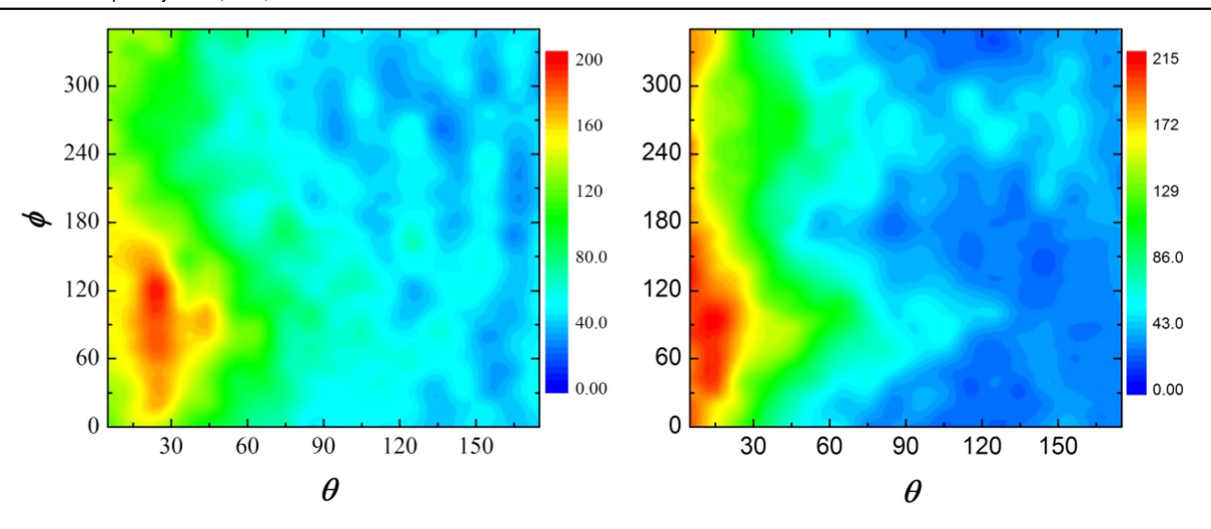


Figure 2. Three-dimensional angular distribution of the electron sum momentum as a function of the azimuthal (y-axis) and polar (x-axis) electron-pair angle. Spectra are shown for an electron sum energy fixed at 10 ± 3 eV (50 ± 7.5 eV) and a transverse momentum transfer fixed at 5 ± 1 a.u. (15 ± 3 a.u.) in the left and right panel, respectively.

As noted above, one of the most important aspects of the capture step is that it selects relatively close collisions so that the NN interaction becomes very important. This leads to average q's which are about an order of magnitude larger than for SI. On the other hand $\mathbf{P_{el}}$ is only about 1–2 a.u. so most of the momentum transferred by the projectile to the target atom is picked up by the recoil ion rather than the electrons. Under these circumstances, it is hard to think of any reason why $\mathbf{P_{el}}$ would be particularly correlated with \mathbf{q} , i.e. one might expect the binary/recoil double lobe structure, which is characteristic of SI, to be strongly washed out, if present at all, for T112, especially for large q.

The spectra of figure 2 show that the correlation between P_{el} and q is indeed weaker than for single ionization, where the binary/recoil double lobe structure is considerably more pronounced. Nevertheless, a surprisingly strong correlation remains. For $\Sigma E_{\rm el} = 10 \, {\rm eV}$ a peak structure, which resembles the binary peak, is observed at $\phi = 90^{\circ}$ and $\theta = 25^{\circ}$, i.e. the direction of P_{eltr} coincides with q_{tr} (which defines $\phi = 90^{\circ}$). In the θ -dependence, this structure is shifted in the forward direction relative to q. However, this shift can partly be explained by the post-collision interaction (PCI) between the outgoing projectile and the continuum electrons, which is known to lead to similar shifts in SI for large η as well. For $\Sigma E_{\rm el} = 50 \, {\rm eV}$ essentially no correlation between ${\bf P_{el}}$ and ${\bf q}$ is visible anymore in the θ -dependence of the cross sections. However, in the ϕ -dependence, such a correlation is even more pronounced than for $\Sigma E_{\rm el} = 10 \, {\rm eV}$. A narrow line of maximized intensity is observed along $\phi=90^{\circ}$ for θ between 0 and approximately 120°. This shows that with large probability the transverse component of P_{el} coincides with q_{tr} . Even more surprising, a corresponding line is also observed for $\phi = 270^{\circ}$, where in SI the recoil peak is usually found.

In order to analyze the azimuthal dependence of the cross sections in more detail in figure 3, we show projections of the 3D plots for $\theta = 90^{\circ} \pm 5^{\circ}$ onto the ϕ -axis for $\Sigma E_{\rm el} = 10 \, {\rm eV}$ (left panel) and 50 eV (right panel).

Two features in these spectra should be emphasized. First, the peak structure at $\phi = 90^{\circ}$ (which for simplicity and in analogy to SI we call binary peak) is narrower and more pronounced for $\Sigma E_{\rm el} = 50\,{\rm eV}$. This is surprising because in this case the transverse component of the recoil momentum, ${\bf p_{rectr}} = {\bf q_{tr}} - {\bf P_{eltr}}$, is much larger than for $\Sigma E_{\rm el} = 10\,{\rm eV}$, so one would expect a weaker correlation between ${\bf P_{eltr}}$ and ${\bf q_{tr}}$. Second, while for $\Sigma E_{\rm el} = 10\,{\rm eV}$ a shallow minimum is seen at $\phi = 270^{\circ}$, a pronounced maximum (corresponding to the recoil peak in SI) is observed for $\Sigma E_{\rm el} = 50\,{\rm eV}$. Thereby, the ϕ -dependence of the cross sections looks almost identical to the double lobe structure which is characteristic of SI. Essentially, the same features we observed for transfer plus single ionization.

Apart from these similarities between T1I2 and SI, the spectra of figure 3 also reveal one important difference: in T1I2 the intensity ratio between the recoil and binary peaks increases with increasing q, while in SI that ratio always sharply drops with increasing q. For q>1 a.u. a recoil peak is usually no longer discernable. A recoil peak almost as tall as the binary peak at q=15 a.u. is therefore a very remarkable feature.

The drastically different q-dependence of the recoil to binary peak ratio suggests that a different mechanism leads to the recoil peak in T1I2 than in SI. In the latter process the recoil peak is often explained in terms of a two-step process. In the first step, the electron is lifted to the continuum by an interaction with the projectile and initially follows the direction of q. In the second step, the electron gets back-scattered by its parent nucleus at 180° so that it is eventually ejected approximately in the direction of -q. To understand the recoil peak in T1I2 we consider another mechanism in which at least two interactions are important and which was originally discussed in the context of SI [1]. Here, the projectile also interacts with the electron (or electron pair) and simultaneously the projectile gets elastically scattered off the target nucleus (for such slow collisions additional interactions may be important as well). Since the longitudinal component of



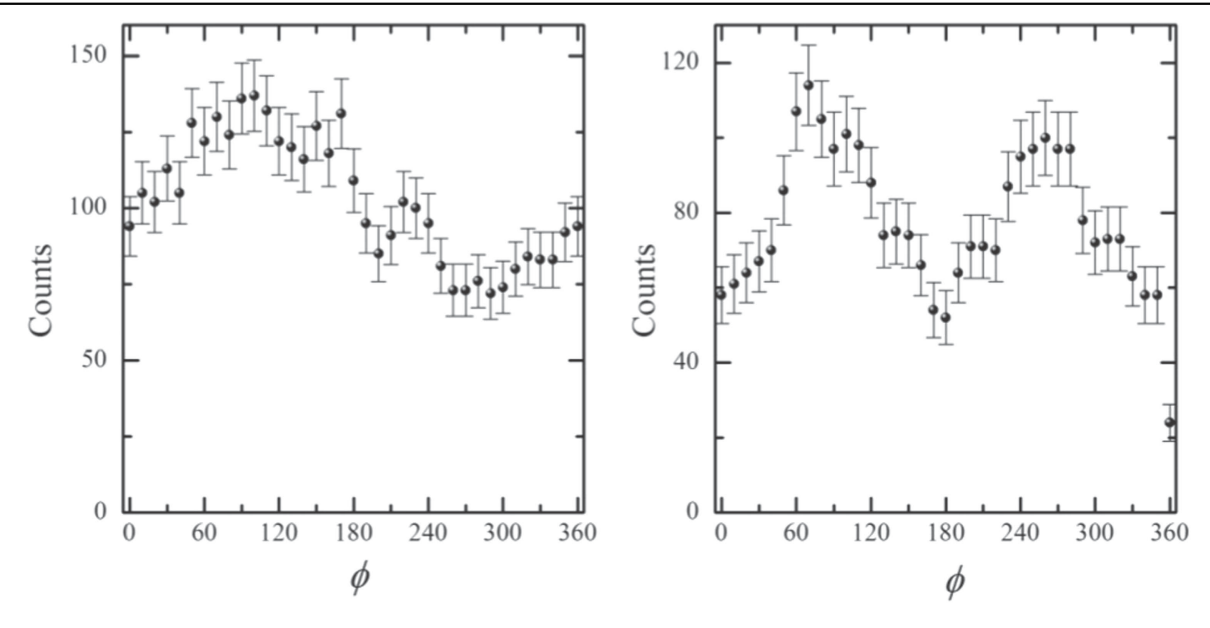


Figure 3. Projections of the three-dimensional angular distributions of figure 2 for $\theta = 90^{\circ}$ onto the azimuthal angular axis. The kinematic parameters for the left and right panels are the same as for figure 2.

the momentum exchange in elastic scattering is zero, the effect of the NN interaction is that q gets rotated azimuthally about the beam axis. If the NN interaction is strong enough this can result in a rotation of 180° so that P_{eltr} ends up pointing in the direction of -q_{tr}. However, one weakness of this explanation is that it should also lead to an enhanced flux for a rotation of 90°, i.e. for $\phi = 180^{\circ}$, while in the data we observe a minimum at that angle separating the binary and recoil peaks from each other. On the other hand, we note that a similar dilemma exists for the accepted explanation for the recoil peak in SI. There, it is also hard to understand why the back-scattering of the electron from the parent nucleus so strongly favors 180°. In the case of SI this apparent conflict is resolved in quantum-mechanical calculations by a superposition of different partial waves leading to a minimum separating the binary and recoil peaks. In the case of T1I2 a final explanation of the recoil peak probably also has to await the full quantum-mechanical treatment.

The analysis of P_{el} shows that the combined ejected electron pair still reveals a surprisingly strong correlation with q. As a next step, we investigate to what extent such a correlation even exists for individual electrons. Furthermore, by analyzing individual electrons, information about potential electron-electron correlation effects can be extracted. To this end, in figure 4 we show FDCS for both electrons, each with an energy of 10 ± 5 eV, ejected into the scattering plane as a function of both polar angles. The transverse momentum transfer is fixed at $q_{\rm tr}=5\pm1$ a.u. Here, we are using different angular coordinates, where ϕ only covers the range [0, 180°] (and $\phi = 90^{\circ}$ represents the scattering plane) and θ covers the range $[-180^{\circ}, 180^{\circ}]$. $\theta = 0$ corresponds to the forward direction, $\theta = 90^{\circ}$ coincides with the direction of q_{tr} and $\theta = -90^{\circ}$ with the direction of $-\mathbf{q_{tr}}$. The horizontal and vertical arrows indicate for each axis the directions of q (positive angles) and -q (negative angles).

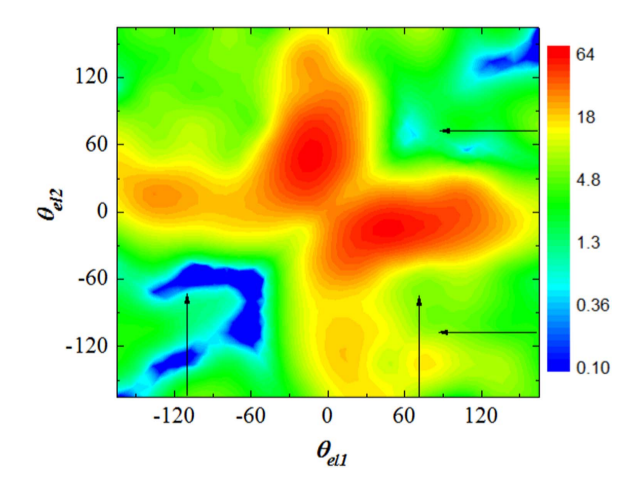


Figure 4. Fully differential cross sections for two electrons, each with an energy of $10\pm5\,\mathrm{eV}$, ejected into the scattering plane (spanned by the initial projectile momentum and the momentum transfer) as a function of the polar ejection angles of both electrons. The transverse momentum transfer was fixed at 5 ± 1 a.u.

It should be noted that the shape of the FDCS plotted in figure 4 can be significantly affected by the multi-hit deadtime, i.e. the minimum time difference between the two electrons hitting the detector for which the detector signals can still be identified as two separate signals. We tested this influence by discarding events for which the two electrons hit the detector within 20, 30, or 40 ns. We found that the deadtime only has a significant effect on the shape of the FDCS along the diagonal for which $\theta_{\rm el1}=\theta_{\rm el2}$.

The coarse structures in figure 4 are a nearly horizontal and a nearly vertical line of maximized intensity occurring near $\theta = 0$. This is a very different shape from what was observed for DI of helium by fast electron impact. There, the spectra were dominated by diagonal lines of maximized intensity, which are characteristic of a correlated DI mechanism [13]. There, the projectile only interacts directly with



one electron. The second electron is then ejected by an interaction with the first electron. For the relatively small projectile speed and the large perturbation parameter $\eta=1.8$ for the present collision system, this correlated mechanism is expected to be weak. Rather, the projectile is more likely to eject both electrons directly in two independent interactions. In the following paragraphs we therefore attempt to interpret the data based on an independent electron model (IEM).

To begin the discussion we recall that in SI, for large values of η , there are three scenarios which the ejected electrons prefer: they like to follow \mathbf{q} (binary peak) or $-\mathbf{q}$ (recoil peak), and they like to be ejected in the forward direction under the influence of PCI. If the ejection of both electrons is independent of each other, one might expect to see the possible combinations of the scenarios of SI in figure 4. This is indeed what we observe: if we follow, for example, the horizontal line of maximized intensity, where electron 2 is ejected nearly in the forward direction, we find maxima near the direction of -q (i.e. electron 1 is in the recoil peak), near $\theta = 0$ (both electrons are ejected in the forward direction), and near the direction of \mathbf{q} (electron 1 is in the binary peak). For the vertical line the corresponding features are observed as well. Therefore, the FDCS plotted in figure 4 strongly suggest that not only P_{el} , but even the individual electron momenta are significantly correlated with q. This is a very surprising observation because one would expect that integration over the momentum transferred to the recoil ion (which is very large due to the capture step) and the other electron momentum would strongly weaken any such correlation.

In a classical picture, this correlation between the electrons and ${\bf q}$ could be explained if typical impact parameters b were larger than the size of the target atom (≈ 1.4 a.u.), in which case the force of the projectile on all target fragments would be acting nearly along the same axis. However, for q=15 a.u. (where the electron momenta are small compared to the recoil-momentum) the impact parameter can be estimated classically using two-body scattering. For an effective screened target charge of 3 (using a Thomas–Fermi potential) we find $b\approx 0.7$ a.u. Furthermore, the correlation seems to get more pronounced with increasing q, i.e. with decreasing b, which also speaks against such a classical picture. At present, we cannot offer any explanation for this observation.

As a final note, we point out that the determination of both the target and the projectile charge state in the experiment rules out the possibility that more than one electron is captured by the projectile or more than two electrons are ejected to the continuum. Therefore, electronic transitions not identified by the experiment are restricted to excitation only. Due to the small excitation energy, except for inner shell electrons, for which the excitation cross section is small, such transitions do not have a significant effect on the momentum balance of the collision. Therefore, the role of the electrons remaining on the target does not go significantly beyond screening the nuclear charge of the target.

In summary, we have measured FDCS for electron capture and ionization of two additional electrons from the target in 30 keV amu⁻¹ He²⁺ + Ar collisions. The sum electron momentum and, even more remarkable, the individual electron momenta are surprisingly strongly correlated with the total momentum transfer, although most of the momentum transferred by the projectile is actually picked up by the recoil ion. Overall, to a large extent the features observed in the FDCS can be explained within an independent electron model. However, some questions remain unanswered and call for rigorous theoretical treatment. In particular it is not clear why the ejected electron momenta follow the momentum transfer so closely.

Acknowledgments

This work is supported by the National Natural Science Foundation of China under Grants No. 11504387, No. 10979007, No. 11274317, and No. 11004202. SFZ thanks the Program of 'One Hundred Talented People' of the Chinese Academy of Sciences for their support. MS is grateful for a visiting professorship from the CAS President's International Fellowship Initiative and for the hospitality of the Institute of Modern Physics. He also acknowledges support from the National Science Foundation under grant No. PHY-1401586. We would like to thank the engineers who operated the 320 kV platform for their assistance in running the ECR ion source.

References

- [1] Schulz M, Fischer D, Kollmus H, Madison D H, Jones S and Ullrich J 2003 *Nature* 422 48
- [2] Rescigno T, Baertschy M, Isaacs W A and McCurdy C E 1999 Science 286 2474
- [3] Ehrhardt H, Jung K, Knoth G and Schlemmer P 1986 Z. Phys. D 1 3
- [4] Schulz M and Madison D H 2006 Int. J. Mod. Phys. A 21 3649
- [5] Ren X, Bray I, Fursa D V, Colgan J, Pindzola M S, Pflüger T, Senftleben A, Xu S, Dorn A and Ullrich J 2011 Phys. Rev. A 83 052711
- [6] Amami S, Ulu M, Ozer Z N, Yavuz M, Kazgoz S, Dogan M, Zatsarinny O, Bartschat K and Madison D H 2014 Phys. Rev. A 90 012704
- [7] Godunov A L et al 2005 Phys. Rev. A 71 052712
- [8] Schöffler M S, Chuluunbaatar O, Popov Y V, Houamer S, Titze J, Jahnke T, Schmidt L P H, Jagutzki O, Galstyan A G and Gusev A A 2013 Phys. Rev. A 87 032715
- [9] Schulz M et al 2012 Phys. Rev. Lett. 108 043202
- [10] Schneider K, Schulz M, Wang X, Kelkar A, Grieser M, Krantz C, Ullrich J, Moshammer R and Fischer D 2013 Phys. Rev. Lett. 110 113201
- [11] Schöffler M S, Godunov A L and Schmidt-Böcking H 2005 J. Phys. B: At., Mol. Opt. Phys. 38 L123
- [12] Zhang R T et al 2013 Phys. Rev. A 87 012701
- [13] Dorn A, Moshammer R, Schröter C D, Zouros T J M, Schmitt W, Kollmus H, Mann R and Ullrich J 1999 Phys. Rev. Lett. 82 2496
- [14] Lahmam-Bennani A, Duguet A, Dal Cappello C, Nebdi H and Piraux B 2003 Phys. Rev. A 67 010701 (R)



- [15] Fischer D et al 2003 Phys. Rev. Lett. 90 243201
- [16] Schulz M, Moshammer R, Schmitt W, Kollmus H, Mann R, Hagmann S, Olson R E and Ullrich J 2000 Phys. Rev. A 61 022703
- [17] Ma X et al 2011 Phys. Rev. A 83 052707
- [18] Ford M J, Moore J H, Coplan M A, Cooper J W and Doering J P 1996 Phys. Rev. Lett. 77 2650
- [19] Madison D H, Schulz M, Jones S, Foster M, Moshammer R and Ullrich J 2002 J. Phys. B: At., Mol. Opt. Phys. 35 3297
- [20] Schulz M et al 2013 Phys. Rev. A 88 022704
- [21] Schulz M, Moshammer R, Perumal A N and Ullrich J 2002 J. Phys. B: At., Mol. Opt. Phys. 35 L161
- [22] Fischer D, Moshammer R, Schulz M, Voitkiv A and Ullrich J 2003 J. Phys. B: At., Mol. Opt. Phys. 36 3555